

1 Mapping SARS-CoV-2 Antibody Epitopes in COVID-19 Patients with a 2 Multi-Coronavirus Protein Microarray

3
4 David Camerini^{1,2}, Arlo Z. Randall¹, Krista Trappi-Kimmons¹, Amit Oberai¹, Christopher Hung¹,
5 Joshua Edgar¹, Adam Shandling¹, Vu Huynh¹, Andy A. Teng¹, Gary Hermanson¹, Jozelyn V.
6 Pablo¹, Megan M. Stumpf³, Sandra N. Lester³, Jennifer Harcourt³, Azaibi Tamin³, Mohammed
7 Rasheed³, Natalie J. Thornburg³, Panayampalli S. Satheshkumar³, Xiaowu Liang¹, Richard B.
8 Kennedy⁴, Angela Yee¹, Michael Townsend^{3*} and Joseph J. Campo^{1*}

9
10 ¹Antigen Discovery Incorporated (ADI), Irvine CA; ²University of California, Irvine, CA; ³Centers
11 for Disease Control and Prevention, Atlanta, GA; ⁴Mayo Clinic, Rochester, MN; *co-senior
12 authors.

13 14 Abstract

15 The emergence and rapid worldwide spread of SARS-CoV-2 has accelerated research and
16 development for controlling the pandemic. A multi-coronavirus protein microarray was created
17 containing full-length proteins, overlapping protein fragments of varying lengths and peptide
18 libraries from SARS-CoV-2 and four other human coronaviruses. Sera from confirmed COVID-19
19 patients as well as unexposed individuals were applied to multi-coronavirus arrays to identify
20 specific antibody reactivity. High level IgG, IgM and IgA reactivity to structural proteins S, M and
21 N, as well as accessory proteins, of SARS-CoV-2 were observed that was specific to COVID-19
22 patients. Overlapping 100, 50 and 30 amino acid fragments of SARS-CoV-2 proteins identified
23 antigenic regions. Numerous proteins of SARS-CoV, MERS-CoV and the endemic human
24 coronaviruses, HCoV-NL63 and HCoV-OC43 were also more reactive with IgG, IgM and IgA in
25 COVID-19 patient sera than in unexposed control sera, providing further evidence of immunologic
26 cross-reactivity between these viruses. The multi-coronavirus protein microarray is a useful tool
27 for mapping antibody reactivity in COVID-19 patients.

28 29 Introduction

30 A novel human coronavirus, which causes severe acute respiratory syndrome, now known as
31 SARS-CoV-2 emerged in December 2019. Infection with SARS-CoV-2 spread rapidly worldwide
32 and on March 11th, 2020, it was declared a pandemic by the World Health Organization (WHO;
33 1). As of November 30th, 2020, there are over 63 million confirmed cases of coronavirus disease
34 (COVID-19) caused by this new virus, resulting in more than 1.4 million deaths, corresponding to
35 a case mortality rate of ~2.3% (2). Best current estimates indicate that SARS-CoV-2 has a basic
36 reproductive number, R_0 , of 2 to 2.5 and an incubation time of approximately 4.6 days (3, 4),
37 which allows rapid spread of the virus. Diagnosis, treatment and vaccination against COVID-19
38 will all benefit from a clear understanding of the immune response to SARS-CoV-2 infection.

39 Previous studies have shown that COVID-19 patients rapidly seroconvert to SARS-CoV-2 and
40 produce IgM, IgG and IgA antibodies directed to several viral proteins (5-8). Reinfection challenge
41 studies in rhesus macaques showed that the humoral and cellular immune response to SARS-
42 CoV-2 infection was effective in blocking reinfection (25, 26). Nevertheless, it is not clear whether
43 all antibody responses are beneficial or whether some antibody responses to SARS-CoV-2 lead
44 to a less favorable course of disease (9, 10). Moreover, enhancement of infection by antibodies

45 has been reported for severe acute respiratory syndrome coronavirus (SARS-CoV), which is
46 closely related to SARS-CoV-2 (11-13, 24).

47 We have created and used a multi-coronavirus protein microarray, containing over one-thousand
48 coronavirus proteins, protein fragments and peptides to map IgG, IgA and IgM antibody epitopes
49 in sera from COVID-19 patients. Our approach localizes the antibody reactivity of COVID-19
50 patients within SARS-CoV-2 proteins and allows us to map the antigenic regions bound.
51 Furthermore, we can similarly measure the antibody reactivity of COVID-19 patients and healthy
52 controls with endemic human coronaviruses and with the two previous epidemic coronaviruses,
53 SARS-CoV and Middle East Respiratory Syndrome coronavirus (MERS-CoV). Our findings and
54 the multi-coronavirus protein microarray we created will be useful in discerning which *de novo*
55 and cross-reactive antibody responses to SARS-CoV-2 are protective and which may be less
56 useful in preventing disease or may even be detrimental. In addition, if high levels of antibody to
57 specific epitopes are found to be especially protective, the array could be used to screen
58 convalescent plasma for therapeutic potential and vaccine recipient sera as a preliminary
59 measure of efficacy (27-30).

60

61 Results

62 The multi-coronavirus protein microarray created and used in this study encompasses over nine-
63 hundred features. It includes the four structural proteins and five accessory proteins of SARS-
64 CoV-2 as well as overlapping 100, 50 and 30 amino acid (aa) protein fragments of these nine
65 SARS-CoV-2 proteins. It also contains the structural proteins of SARS-CoV, MERS-CoV, HCoV-
66 NL63 and HCoV-OC43, plus overlapping 13-20 aa peptides of the SARS-CoV structural proteins
67 and of the S proteins of MERS-CoV, HCoV-NL63 and HCoV-OC43 (Table 1).

Table 1. Features of the 1st Generation ADI Multi-Coronavirus Protein Microarray

Virus	S-protein	E-protein	M-protein	N-protein	Accessory or Other Proteins	Total Number of Features = 934
SARS-CoV-2	RBD*, S [#] from BEI, S1, S2, 30, 50 & 100 aa fragments by IVTT at ADI	Protein and 30, 50 aa fragments by IVTT at ADI	Protein and 30, 50, 100 aa fragments by IVTT at ADI	Protein BEI, 30, 50 & 100 aa fragments by IVTT at ADI	ORF 3a, 6, 7a, 8 and 10 protein, 30, 50 & 100 aa fragments by IVTT at ADI	12 proteins, 310 fragments = 322 features
SARS-CoV	Protein** and peptide set from BEI Resources	IVTT by ADI, peptides from BEI	Protein, peptides from BEI	Protein, peptides from BEI	3CL protease	5 proteins, 265 peptides = 270 features
MERS-CoV	BEI Resources	IVTT by ADI	IVTT by ADI	BEI Resources	ORF 3a, 4a, 4b, 5 and 8b protein IVTT by ADI	9 proteins
HCoV-NL63	Protein by IVTT at ADI, peptides from BEI	IVTT by ADI	IVTT by ADI	IVTT by ADI	ORF 3 protein IVTT by ADI	5 proteins and 96 peptides = 101 features
HCoV-OC43	Protein by IVTT at ADI, peptides from BEI	IVTT by ADI	IVTT by ADI	IVTT by ADI	HE, N2 protein IVTT by ADI	6 proteins and 226 peptides = 232 features

IVTT means coupled *in vitro* transcription and translation. * RBD is the receptor binding domain, aa 319 to 541 of the SARS-CoV-2 S protein. # SARS-CoV-2 S protein is a stabilized form with a trimerization sequence and transmembrane domain deletion. ** SARS-CoV-S protein is a transmembrane domain deleted form.

68

69 The multi-coronavirus array was incubated with sera from two sets of patient samples and
70 associated negative controls collected in different regions of the USA. The first set of sera from

71 ten COVID-19 patients and ten pre-pandemic healthy donors was obtained from the Centers for
72 Disease Control and Prevention (CDC) in Atlanta, Georgia. The second set included sera from
73 ten COVID-19 patients and nine pre-pandemic samples obtained from the Mayo Clinic in
74 Rochester, Minnesota. The age, sex and SARS-CoV-2 ELISA result of the COVID-19 patient and
75 healthy control blood donors in both sample sets is shown in Tables 2 and 3. ELISA's were
76 performed separately at the two different sites and discriminated the COVID-19 patient samples
77 from the control samples.

78

79

80 **Table 2 Serum Donors for Samples Obtained from the CDC**

Sample ID	SARS-CoV-2 S ELISA (S/T)	Age Decade	Sex
C1	0.25	60's	M
C2	0.09	20's	M
C3	0.18	40's	M
C4	0.34	50's	M
C5	0.19	60's	M
C6	0.94	40's	M
C7	0.26	40's	M
C8	0.15	50's	M
C9	0.40	40's	M
C10	0.19	50's	M
P1	2.06	60's	F
P2	3.98	60's	M
P3	5.47	50's	F
P4	2.35	20's	F
P4	5.16	70's	F
P6	5.21	70's	M
P7	3.82	30's	M
P8	5.30	80's	M
P9	3.81	40's	F
P10	5.20	40's	M

81 S/T = signal/threshold for positivity ratio; >1.0 is positive

82 C = healthy negative control; P = COVID-19 patient

83

84 **Table 3. Serum Donors for Samples Obtained**
85 **from the Mayo Clinic**

Sample ID	SARS-CoV-2 S ELISA (S/C)	Age Decade	Sex
C101	NA	10's	M
C102	NA	10's	F
C103	NA	10's	M
C104	NA	10's	M
C105	NA	10's	M
C106	NA	10's	M
C107	NA	10's	F
C108	NA	10's	F
C109	NA	20's	F
P101	2.76	50's	F
P102	3.71	50's	M
P103	3.83	70's	M
P104	1.42	30's	M
P105	4.24	10's	F
P106	2.48	40's	F
P107	1.5	50's	F
P108	3.05	60's	F
P109	2.03	70's	M
P110	3.6	70's	M

86 S/C = signal/calibrator ratio; >1.1 is positive

87 C = healthy negative control; P = COVID-19 patient

88 NA = not applicable

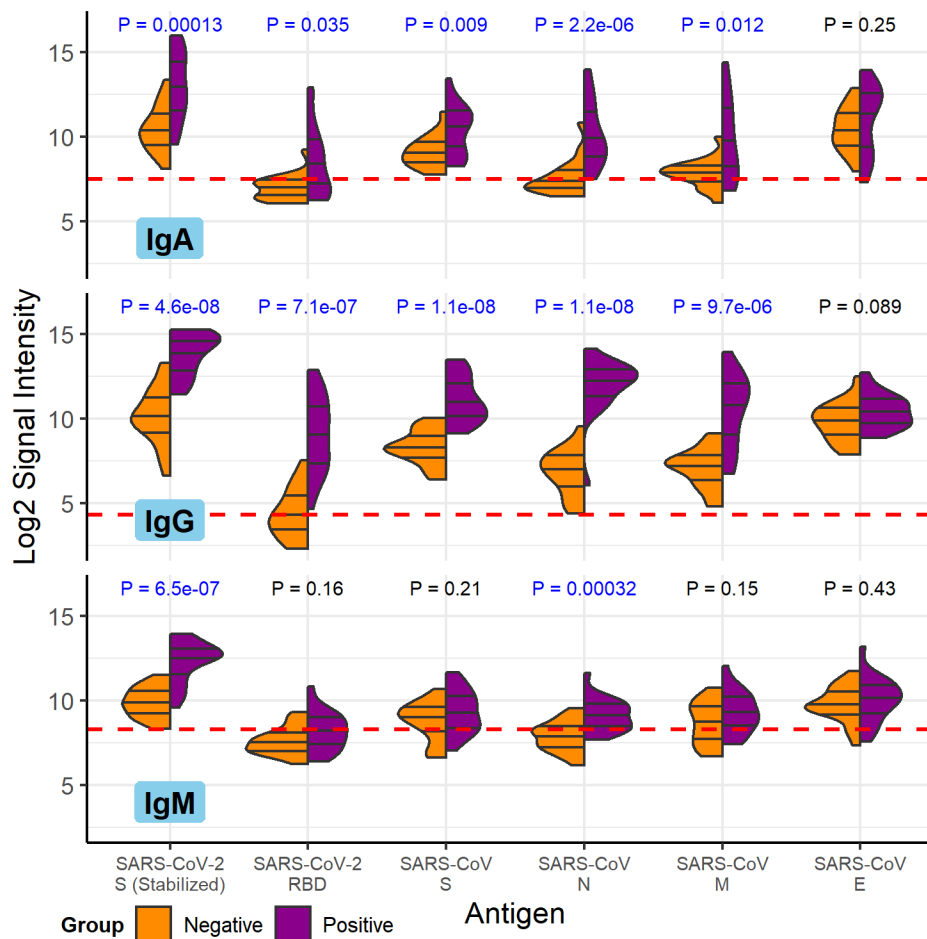
89

90

91 **Specific antibody reactivity to SARS-CoV-2 and SARS-CoV purified recombinant proteins**
92 **in COVID-19 patients**

93 The specimens from COVID-19 patients had robust anti-SARS-CoV-2 IgG and IgA antibodies.
94 IgM antibody responses were weaker. The magnitude and specificity of the antibody responses
95 were similar in both sets of samples, so they are presented together here. COVID-19 patient
96 serum IgG, IgA and IgM reacted strongly to purified SARS-CoV-2 spike (S), as well as SARS-
97 CoV nucleocapsid (N), S and membrane (M) proteins compared to healthy control sera (Fig. 1).
98 The receptor binding domain of the SARS-CoV-2 S protein (RBD) had overall weaker antibody
99 binding signals, but nevertheless was significantly more reactive in COVID-19 patient serum IgG
100 and IgA. The signals shown in figure 1 are the base two logarithm of the raw intensities without
101 normalization, since the background reactivity of each purified protein is different. The SARS-
102 CoV-2 S and RBD as well as the SARS-CoV S, N and M purified proteins had the largest mean

103 differences between IgG binding of the negative and positive groups, and the differences are the
 104 most statistically significant (t-test p values $<10^{-5}$). The same five antigens had the largest
 105 significant mean differences between IgA binding of the negative and positive groups. Only
 106 SARS-CoV-2 S and SARS-CoV N, however, had significant differential IgM binding between the
 107 COVID-19 patients and the control group. These results are in agreement with the enzyme linked
 108 immunosorbent assays (ELISA) shown in Tables 2 and 3.

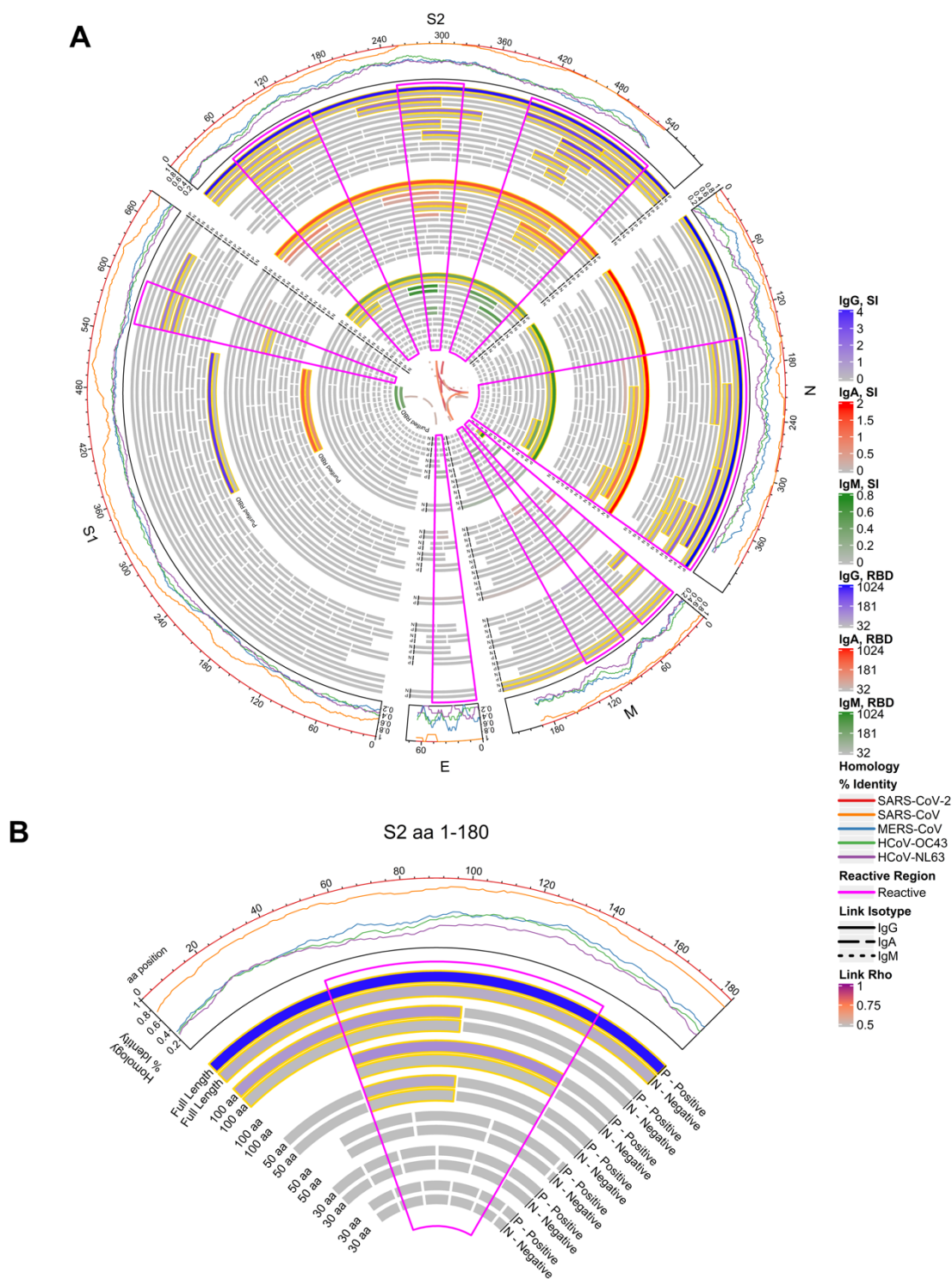


109
 110 **Figure 1. COVID-19 patient and healthy control antibody reactivity with purified SARS-CoV-**
 111 **2 and SARS-CoV proteins.** The split violin plot shows the \log_2 -transformed fluorescence signal
 112 intensity distribution of antibodies bound to each purified protein on the multi-coronavirus protein
 113 microarray. Within each half-violin are three lines representing the interquartile range and the
 114 median. Above each split violin is the Wilcoxon rank sum p value, colored blue for significant p
 115 values below 0.05. The three panels are split by isotype (IgG, top; IgA, middle; IgM, bottom).
 116 Horizontal red dashed lines are drawn at the median of all signal intensities against purified
 117 proteins ($n=14$) and peptides ($n=587$) plus 1.0, i.e. double the global median—this threshold
 118 serves as a point of reference, but not necessarily a seropositivity cutoff for each protein.

119
 120 **SARS-CoV-2 protein fragments identify antigenic regions**

121 Nine SARS-CoV-2 full-length proteins were produced by coupled *in vitro* transcription and
 122 translation (IVTT): S, envelope (E), M, N, open reading frames (ORF's) 3a, 6, 7a, 8 and 10. We
 123 used the same technique to produce overlapping 100 amino acid (aa), 50 aa and 30 aa fragments

124 of each of these nine SARS-CoV-2 proteins and to produce the structural proteins and some
125 accessory proteins of HCoV-NL63, HCoV-OC43 and MERS-CoV. Using aa start and end
126 positions of each fragment within the protein, differential reactivity between the COVID-19 and
127 healthy donor groups was mapped in a circular heatmap for the structural proteins (Fig. 2). This
128 analysis allowed us to identify antigenic regions in each SARS-CoV-2 structural protein. The
129 SARS-CoV-2 N protein showed the strongest reactivity in its carboxy terminal 100 aa fragment,
130 as well as in 50 aa fragments covering the same region. This region was recognized by IgG, IgA
131 and IgM with significant differential reactivity between COVID-19 patients and the healthy control
132 group. The middle of the N protein also had a region recognized by IgG and IgA identified by two
133 100 aa fragments. Together these antibody-reactive regions encompass about two thirds of the
134 N protein that likely contains at least two epitopes. The S1 protein also showed greatest IgG
135 binding near its carboxy terminus, in the penultimate 100 aa fragment. This antigenic region of
136 S1 was defined further by IgG and IgA reactivity with 50 aa fragments from aa 550 to 600. The
137 region containing the RBD was not strongly reactive when produced by IVTT. In contrast, the S2
138 protein of SARS-CoV-2 showed three regions of strong IgG, IgA and IgM binding and differential
139 reactivity with full-length, 100 aa and 50 aa fragments. Only the region near the carboxy terminus,
140 however, was also reactive as a 30 aa fragment. This reactive 30 aa fragment, from aa 450 to
141 480 of S2 (1,135 to 1,165 of S), therefore likely defines a linear IgG epitope in this highly antigenic
142 protein. Notably, an epitope in the central S2 antigenic region was differentially reactive for IgG
143 and IgA, but showed equal levels of IgM reactivity in 100 aa and 50 aa fragments, perhaps
144 indicating a region of cross-reactivity for IgM produced by memory B cells. An additional short
145 epitope was found in the amino terminal 30 aa fragment of the SARS-CoV-2 M protein. This short
146 fragment was highly reactive with COVID-19 patient serum IgG compared to healthy donor serum
147 IgG, while larger fragments containing it and indeed the full-length M protein were not as highly
148 discriminatory for COVID-19 patient sera. The SARS-CoV-2 E protein had only one 30 aa
149 fragment that showed low-level reactivity with IgA and IgM, in both COVID-19 positive and
150 negative control groups. The antigenic regions of SARS-CoV-2 structural proteins we identified
151 were not associated with higher or lower levels of homology between SARS-CoV-2 and other
152 human coronaviruses (percent aa sequence identity shown in outer track of Fig. 2). There was a
153 moderate to high level of correlation between antibody reactivity with S2, N and M proteins
154 produced *in vitro*, particularly for IgG (Pearson's correlation coefficient shown in inner links of Fig.
155 2). Less reactivity was seen in non-structural proteins, but significant reactivity of COVID-19
156 patient sera compared to control sera could be identified in fragments of the 3a and 7a accessory
157 proteins (Supplemental Figure 1).



158

159 **Figure 2. Reactivity of COVID-19 patient and healthy donor IgG (outer band of bars), IgA**

160 **(middle band) and IgM (inner band) to SARS-CoV-2 proteins and protein fragments. (A)** The

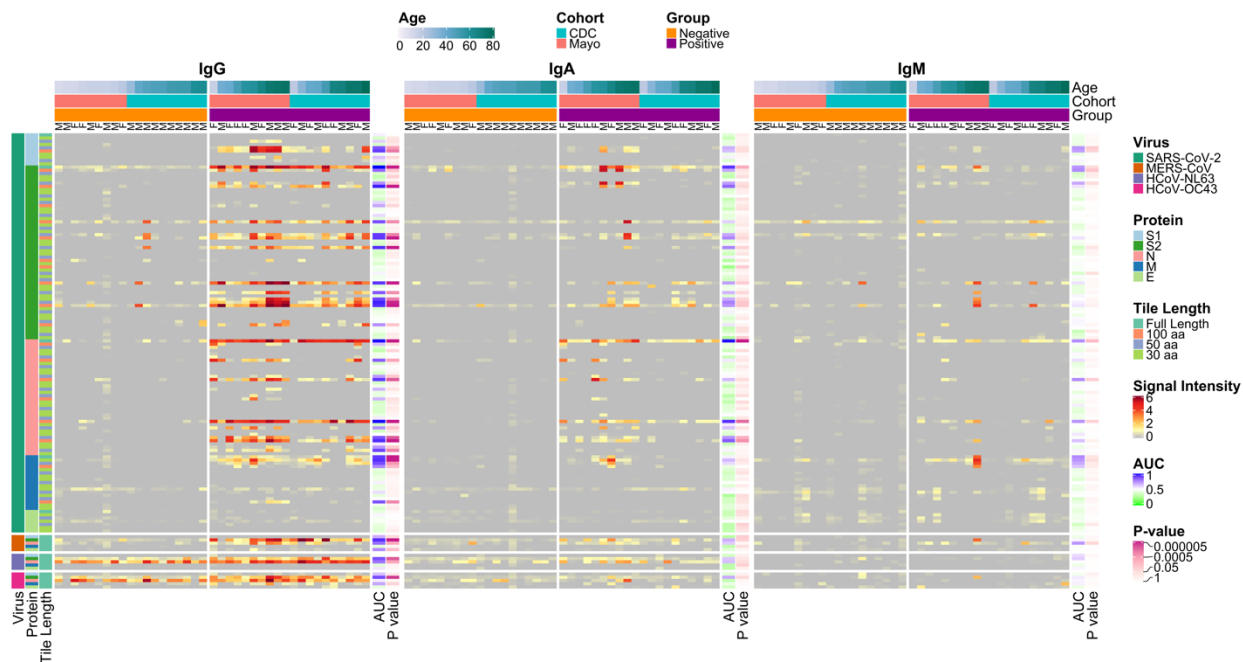
161 circular graphic maps the amino acid (aa) position of SARS-CoV-2 fragments, showing a heat

162 map of antibody levels in each group for overlapping regions of different aa length. Proteins are

163 indicated outside the circle plot followed by a line graph showing the sequence homology of other
 164 CoVs with SARS-CoV-2 for each gene. Proteins and protein fragments produced *in vitro* are
 165 indicated by bars and show length and position of each fragment in each protein. Each fragment
 166 is drawn twice and shows group mean normalized signal intensity of antibody binding to each
 167 fragment for COVID-19 patient samples (P) and negative control sera (N). The purified receptor
 168 binding domain (RBD) is additionally shown for comparison. Signal intensity is shown by color
 169 gradients: IgG (grey to blue), IgA (grey to red), and IgM (grey to green). Bar pairs shown with gold
 170 outline represent significantly differential antibody binding between COVID-19 patients and
 171 healthy controls, defined as a mean signal intensity ≥ 0.1 in at least one group and a t-test p value
 172 ≤ 0.05 . The regions of greatest reactivity for each protein are outlined in magenta. Some
 173 fragments in E and M proteins that meet the reactivity threshold (grey) and are better visualized
 174 by individual responses as shown in Fig. S2. The Pearson's correlation coefficients ("Rho")
 175 between each full-length protein for each isotype are shown as links between protein sectors in
 176 the center of the circle (IgG: solid links, IgA: dashed, IgM: dotted). **(B)** A slice of the circular
 177 graphic is amplified and labeled in more detail as a guide to interpreting the full figure. The first
 178 180 aa sequence of S2 is shown for IgG only.
 179

180 **Individual antibody response profiles to antigenic regions of SARS-CoV-2 and other**
 181 **human coronaviruses**

182 Individual responses to the antigenic regions of SARS-CoV-2 proteins identified by reactivity with
 183 protein fragments varied substantially, as they did for the structural proteins of other human
 184 coronaviruses (Fig. 3). Responses against the SARS-CoV-2 S1, S2 and N protein fragments, as
 185 well as the 30aa fragments of the M protein are shown in Supplemental Figure 2. Within the
 186 antigenic regions, some fragments, particularly 30 aa fragments, were nonreactive with COVID-
 187 19 patient sera, but others were reactive in a subset of individuals. Heterogeneity was higher and
 188 overall signal intensities were lower for IgA and IgM than for IgG. There were no significant
 189 associations between age and sex with antibody levels in the positive group after adjustment for
 190 the false discovery rate for any of the three isotypes (Supplemental Table 1).



191

192 **Figure 3. Reactivity in COVID-19 positive and negative IgG (left heatmap), IgA (middle**
193 **heatmap) and IgM (right heatmap) to SARS-CoV-2 and other HCoV proteins and protein**
194 **fragments produced *in vitro*.** The heatmaps present the signals of antibody binding to individual
195 proteins and protein fragments within the antigenic regions of SARS-CoV-2, as well as the full-
196 length structural proteins of MERS-CoV, HCoV-NL63 and HCoV-OC43, for individual samples.
197 Columns represent serum samples ordered by increasing age within group and cohort, and rows
198 represent proteins or protein fragments; 128 SARS-CoV-2 proteins or fragments, five proteins
199 each of MERS-CoV, HCoV-OC43 and HCoV-NL63. Antibody signal intensity is shown on a color
200 scale from grey to red. Sample information is overlaid above the heatmaps and includes sex
201 (M/F), group (Negative or Positive), cohort (CDC or Mayo) and age (years). Protein/fragment
202 information is annotated to the left of the heatmaps and includes the virus, full-length protein name
203 and the amino acid length of the protein fragments (“Tile Length”, as full length, 100, 50 or 30 aa).
204 For each isotype, the receiver operating characteristic area under the curve (AUC) and the
205 unadjusted t-test *p* value between negatives and positives are shown to the right of each heatmap.

206

207 Full-length N proteins of the endemic HCoV’s were reactive with IgG from COVID-19 patients and
208 healthy controls. HCoV-NL63 N was significantly reactive (normalized signal intensity ≥ 1.0) with
209 IgG controls and COVID-19 patients (17/19 and 20/20, respectively; proportions test *p* value =
210 0.4) (Fig. 3), while HCoV-OC43 N was significantly reactive with IgG control sera and patient sera
211 (15/19 and 20/20, respectively; $p=0.1$). In contrast, IgG from only two control subjects reacted
212 with the SARS-CoV-2 full length N protein while nearly all of the patients’ serum IgG reacted
213 (19/20; $p=6.8e-7$). Reactivity of the control serum IgG with fragments of the SARS-CoV-2 N
214 protein occurred exclusively in the C-terminal region of the protein (1/19) while COVID-19 patient
215 serum IgG reacted frequently with fragments in the central region (12/20; $p=2.1e-4$) of the protein
216 as well as the C-terminal region (19/20; $p=1.3e-7$).

217

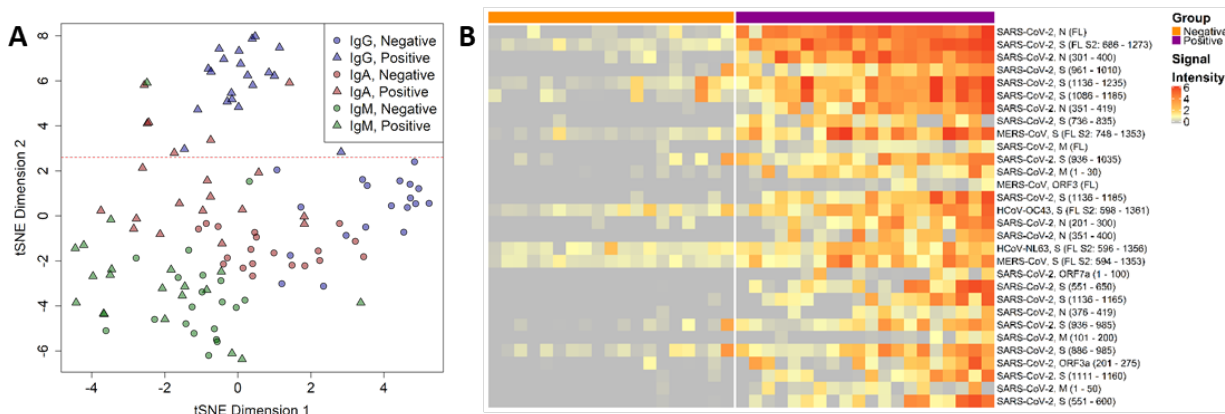
218 The S2 protein was reactive with patient IgG at a much higher frequency than in the controls for
219 both HCoV-NL63 (5/19 and 16/20 positives, respectively; $p=2.4e-3$) and HCoV-OC43 (4/19 and
220 18/20, respectively; $p=5.9e-5$). The higher frequencies in the positives provide strong evidence of
221 increased responses due to their exposure to SARS-CoV-2. Some control subject’s IgG reacted
222 with the C-terminal (4/19) or central regions (4/19) of the SARS-CoV-2 S2 protein but none
223 reacted with the N-terminal region; this includes one individual which had unique reactivity to
224 SARS-CoV-2 S2 fragments 401-500 and 451-550 (Figure S2, G). By ELISA, this serum had a
225 S/C value of 0.94, which was just below the positivity threshold of 1.0 and much higher than other
226 healthy donor sera. This reactivity was unique among healthy donors but did not directly translate
227 to reactivity with OC43 or NL63 FL S proteins. Overall, COVID-19 patient serum IgG reacted with
228 the SARS-CoV-2 S2 protein C-terminal (19/20; $p=1.3e-5$), central (17/20; $p=2.3e-4$), and/or N-
229 terminal (12/20; $p=2.1e-4$) 100 aa fragments much more frequently than healthy donor sera.

230 The reactivity of COVID-19 patient serum IgA compared to IgA of healthy donor sera was similar
231 to results obtained for IgG. The IgA results had lower statistical significance than the IgG results,
232 however, likely due to the lower concentration of IgA in serum compared to IgG. Nevertheless,
233 many of the same proteins were the most differentially reactive with COVID-19 patient serum IgA
234 compared to healthy donor serum IgA, including the N and S proteins and RBD of SARS-CoV-2
235 as well as the N, S and M proteins of SARS-CoV with t-test *p* values ranging from 2.1×10^{-6} to
236 1.1×10^{-3} (Fig. 3). The COVID-19 patient sera used in this study had less coronavirus reactive
237 IgM than IgG or IgA, perhaps because the samples were obtained during the convalescent phase
238 of disease. Nevertheless, significantly greater IgM reactivity was seen in patient sera compared
239 to control donor sera for four proteins and two protein fragments produced *in vitro* (Fig. 3). These
240 were the N, S2 and M proteins of SARS-CoV-2, the MERS-CoV N protein, the carboxy terminal

241 100 aa fragment of the SARS-CoV-2 N protein and the amino terminal 30 aa fragment of the
 242 SARS-CoV-2 M protein.

243 A library of 587 peptides, 15 to 20 aa in length, from the epidemic SARS-CoV (covering S, N, M
 244 and E proteins) and two endemic human coronaviruses (covering S protein) was printed on the
 245 multi-coronavirus microarray at the same concentration as full-length purified recombinant
 246 proteins. The peptides, however, showed lower antibody reactivity than full length proteins or
 247 protein fragments of 30, 50 or 100 aa. Exceptionally, a single 17 aa peptide from HCoV-OC43 S
 248 protein with sequence CSKASSRSAIEDLLFDK spanning residues 905 to 921 had approximately
 249 3.5-fold higher mean reactivity in the COVID-19 patient sera ($p=0.001$, not significant after
 250 adjustment for the false discovery rate). This peptide mapped to the SARS-CoV-2 sequence
 251 PSKPSKRSEFIEDLLFNK at residues 809 to 825 of S protein with identical residues in 12/17
 252 positions.

253 To visualize the relative importance of antibody isotype binding in differentiating COVID-19
 254 positive sera from negative sera, the samples were projected in two dimensions for each isotype
 255 using t-distributed stochastic neighbor embedding (tSNE; Fig. 4A), a nonlinear machine learning
 256 dimensionality reduction method which clusters together similar sets of multidimensional data.
 257 The thirty most reactive proteins for all isotypes were selected for this analysis to reduce the effect
 258 of differing isotype background levels that would be notable in low-reactivity proteins (Fig. 4B).
 259 Each of the isotypes cluster separately, but only IgG gave a clear delineation of positives and
 260 negatives (at ~ 2.6 in tSNE dimension 2). Henceforth, the focus of the presented data is on the
 261 IgG responses.



262
 263 **Figure 4. IgG responses give the best delineation of COVID-19 patient sera from healthy**
 264 **donor sera. (A)** The IgG, IgA and IgM responses against the 30 most reactive IVTT proteins by
 265 mean of all samples and isotypes were projected for each sample across two dimensions using
 266 t-distributed stochastic neighbor embedding (tSNE). Points represent individual samples and are
 267 colored according to the isotype measurement. The shape represents the group in which the
 268 sample belonged, either the “Negative” healthy donor group or the “Positive” COVID-19 patient
 269 group. The horizontal red dashed line ($y=2.6$) separates the IgG responses in negative and
 270 positive individuals. **(B)** The heatmap shows the 30 most differentially reactive IgG responses to
 271 IVTT proteins between the negative and positive groups. Columns represent serum samples,
 272 separated by group with colored headers. Rows represent full-length or fragmented proteins
 273 produced by cell-free expression *in vitro*. The protein annotations to the right of the heatmap
 274 denote the virus, protein and in parentheses the amino acid range of the fragment or full length
 275 “FL” protein. Normalized signal intensity is displayed on a grey to red color scale.

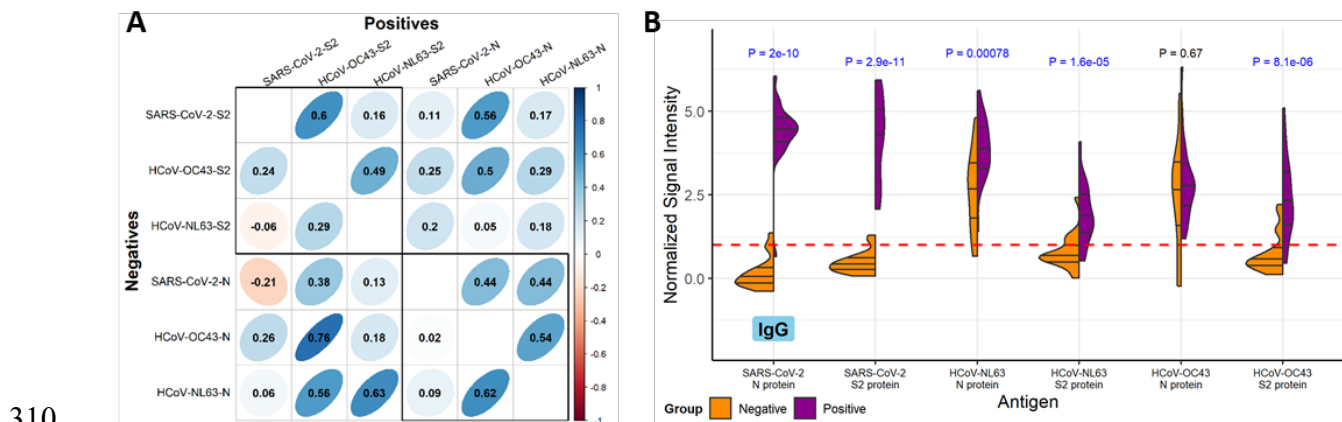
276

277 The full-length SARS-CoV-2 N and S2 proteins as well as several fragments of both proteins had
 278 the top nine largest mean differences in IgG reactivity between COVID-19 patients and healthy
 279 controls (Fig. 4B). These results were also statistically significant with t-test p values ranging from
 280 2.1×10^{-6} to 4.3×10^{-2} (Supplemental Table 1). Antibody responses to HCoV-NL63, HCoV-OC43
 281 and MERS-CoV proteins were also among the thirty most discriminatory antigens for
 282 differentiating COVID-19 patients from control donors due to high reactivity with COVID-19
 283 positive sera, while also demonstrating a considerable reactivity with negative. Nearly all the same
 284 epitopes and regions of reactivity found for IgG were recapitulated by IgA reactivity as well, when
 285 reactivity to the overlapping 100 aa, 50 aa and 30 aa protein fragments was analyzed (Fig. 3).
 286 This includes the epitopes mapped in the SARS-CoV-2 N, S1, S2 and M proteins (Fig. 2).

287

288 Correlation of SARS-CoV-2 and endemic human coronavirus responses

289 By comparing the correlation between antibody responses to the S2 and N proteins of SARS-
 290 CoV-2 with responses to the S2 and N proteins of endemic human coronaviruses, in both COVID-
 291 19 positive and negative sera, we can estimate to what extent antibody responses to SARS-CoV-
 292 2 are the result of *de novo* immune responses or of boosting pre-existing immunity. There were
 293 significantly stronger correlations between SARS-CoV-2 S2 protein IgG and HCoV-OC43 S2
 294 proteins in the positive group (Pearson's correlation coefficient, $\rho=0.6$) than the negative group
 295 ($\rho=0.24$; Fig. 5A, top left). In the negative group, SARS-CoV-2 N protein IgG had no correlation
 296 with HCoV-OC43 N protein ($\rho=0.02$) or HCoV-NL63 N protein ($\rho=0.09$), whereas the correlations
 297 in the positive group were higher (HCoV-OC43 and HCoV-NL63 had $\rho=0.44$ with SARS-CoV-2 N
 298 protein). HCoV-OC43 and HCoV-NL63 N protein reactivity exhibited strong correlations in both
 299 positive and negative groups ($\rho=0.54$ and $\rho=0.62$, respectively). However, S2 protein reactivity
 300 correlations between these endemic human coronaviruses were lower in the negative group than
 301 the positive group ($\rho=0.29$ and $\rho=0.49$, respectively). Further inspection of the correlation
 302 scatterplot matrix (Supplemental Figure 3) showed a clear outlier in the CDC positive group for
 303 SARS-CoV-2 N protein and that correlations may differ if the CDC and Mayo cohorts were
 304 considered separately. Differential IgG reactivity between the COVID-19 positive and negative
 305 groups was also observed with the S2 and N proteins of SARS-CoV-2, HCoV-OC43 and HCoV-
 306 NL63. Positive COVID-19 patient sera had significantly higher IgG levels to S2 and N than the
 307 negative healthy donor sera for all three coronaviruses (Fig. 5B), with the exception of HCoV-
 308 OC43 N protein; this protein also showed higher IgA reactivity in the negatives (Supplemental
 309 Figure 4).



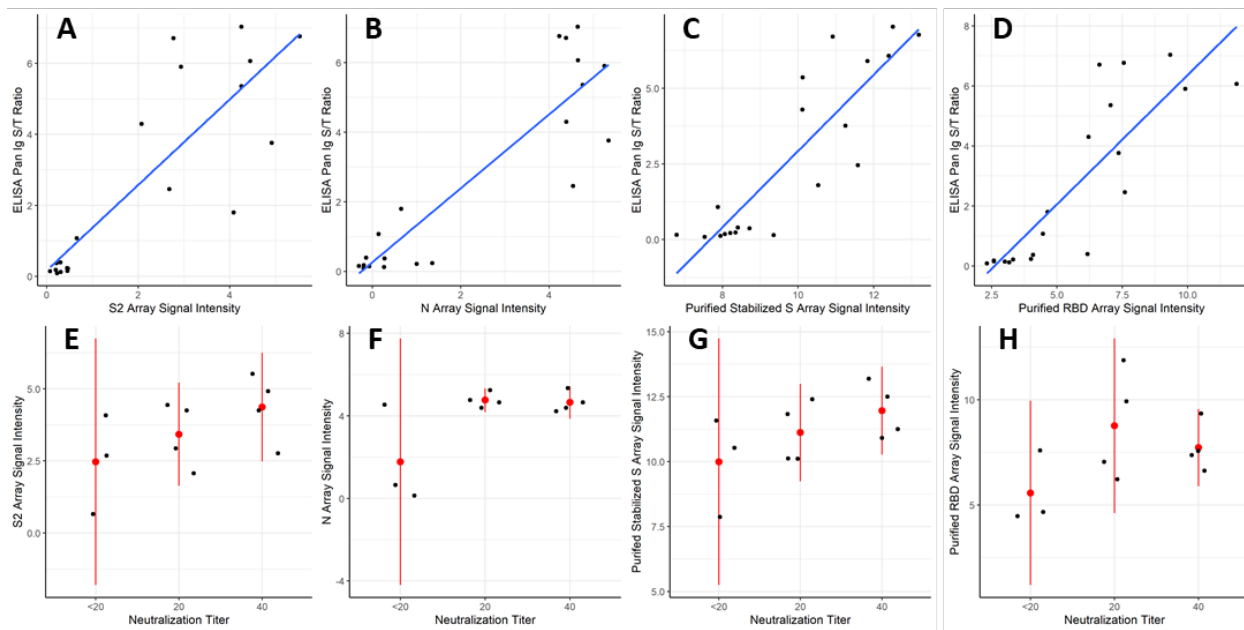
310
 311 **Figure 5. Correlation and concordance between IgG responses to SARS-CoV-2 and**
 312 **endemic human coronavirus N and S2 proteins. (A)** The correlogram shows the Pearson's

313 correlation coefficient (ρ) between IgG normalized signal intensity to SARS-CoV-2, HCoV-OC43
314 and HCoV-NL63 N and S2 full-length proteins produced *in vitro*. The lower half of the diagonal
315 shows correlation between reactivity of sera in the negative group, and the upper half of the
316 diagonal shows the positive group serum correlations. The color scale indicates positive
317 correlation in darker shades of blue and negative correlation in darker shades of red, and ρ is
318 overlaid on each comparison. Additionally, the narrowness and slope of the ellipses represent
319 increasing positive or negative correlation. Boxes are drawn around the intra-S2 and intra-N
320 protein comparison. **(B)** The split violin plot shows the normalized IgG signal intensity distribution
321 for each N and S2 protein produced *in vitro*. Within each half-violin are three lines representing
322 the interquartile range and the median. Above each split violin is the Wilcoxon rank sum p value,
323 colored blue for significant p values below 0.05. The red dashed line represents the 1.0
324 seropositivity cutoff.

325

326 **Correlation of multi-coronavirus protein microarray responses with ELISA and virus** 327 **neutralization assays**

328 S protein-based ELISA results from the CDC cohort, taken on all COVID-19 or healthy donor
329 samples, were compared with IgG reactivity in the protein microarray data by Pearson's
330 correlation coefficient for the highly reactive IVTT S2 protein ($\rho=0.85$), IVTT N protein ($\rho=0.9$),
331 purified recombinant full-length S protein ($\rho=0.88$) and the purified recombinant RBD ($\rho=0.85$),
332 shown in Fig. 6A-D. The data clustered separately for negative responders and positive
333 responders for all proteins. Virus neutralization titers were only available for the CDC COVID-19
334 patients and one healthy donor sample that tested near the 1.0 cutoff for ELISA reactivity ($n=11$).
335 In all cases, neutralization activity was low, with positive neutralization titers at dilution factors of
336 20 or 40. Despite the low values and few samples, a trend was observed using linear regression
337 for IVTT S2 ($\beta=6.5$, $p=0.076$), IVTT N ($\beta=6$, $p=0.036$) and stabilized purified S ($\beta=6.3$, $p=0.077$)
338 (Fig. 6E-H). There was no association, however, of neutralization with responses to IgG reactivity
339 with purified RBD ($\beta=2.8$, $p=0.27$). The linear regression models were specified with values of 0
340 for titers <20 . However, since the true titer is between 0 and 20, neutralization was also modeled
341 as an ordinal variable using ordinal logistic regression. Similar results were obtained for IVTT S2
342 and stabilized purified S, whereas association with IVTT N protein was no longer significant. The
343 complete correlation results for all proteins are shown in Supplemental Table 1.



344
345 **Figure 6. Correlation of IVTT and purified protein microarray results with ELISA and virus**
346 **neutralization assays.** (A-D) The scatter plots show the SARS-CoV-2 S protein-based ELISA
347 Pan Ig signal/threshold ratio (y-axis) against the protein microarray normalized IgG signal intensity
348 for S2 and N proteins produced in vitro, as well as for the stabilized, purified full-length S protein
349 and the purified RBD fragment of S1 protein (x-axis), respectively. The blue lines were fit to the
350 data using linear regression. (E-H) The dot plots show individual values of each patient for the
351 protein microarray normalized IgG binding intensity (y-axis) of the four proteins shown in (A-D) at
352 each neutralization titer (x-axis). Red dots are plotted at the means of each stratum, and the red
353 lines represent the 95% confidence intervals.

354

355 Discussion

356 In this study of twenty COVID-19 patients, the strongest antibody responses to the SARS-CoV-2
357 proteins used on this array, for all antibody isotypes, were directed to the N and S2 proteins as
358 has been previously seen in other studies (5, 8, 14, 15). We also detected antibody responses to
359 S1, M and accessory proteins 3a and 7a. Moreover, we were able to localize regions of each of
360 these SARS-CoV-2 proteins to which antibodies bound, by antibody reactivity with overlapping
361 protein fragments of three different lengths: 100, 50 and 30 aa. Our results were internally
362 consistent in that reactive proteins had more reactive fragments than non-reactive proteins and
363 100 aa reactive fragments contained reactive 50 aa fragments and sometimes they also contained
364 reactive 30 aa fragments. We found little reactivity of COVID-19 patient sera with 13-20 aa
365 peptides from SARS-CoV S, M, E or N, HCoV-OC43 S or HCoV-NL63 S with the exception of
366 one S2 peptide from HCoV-OC43.

367 Many previous publications have predicted B cell epitopes in SARS-CoV-2 proteins using a
368 variety of immunoinformatic approaches (16-19). Crooke *et al.* predicted twenty-six potential
369 linear B cell epitopes in the S protein, fourteen potential epitopes in the N protein, and three
370 potential epitopes in the M protein. We noted antibody reactivity with regions containing some,
371 but not all of these predicted epitopes. In particular, of the top six predicted B cell epitopes in the
372 S protein we found significantly stronger reactivity with COVID-19 patient sera compared to
373 healthy donor sera for regions containing three epitopes: DIADTT, residues 568-573 near the

374 carboxy terminus of S1, PPIKD, residues 792-796 near the amino terminus of S2 and
375 VYDPLQPELDSF, residues 1137-1148 near the carboxy terminus of S2. The other three top
376 predicted B cell epitopes of the S protein, residues 405-428, 440-450 and 496-507, were not in
377 highly reactive regions of the S protein in our experiments, perhaps due to the overall low reactivity
378 of the S1 protein except for its carboxy terminal region or a need for native structure not found in
379 protein fragments produced *in vitro*. Similarly, we found COVID-19 specific reactivity for regions
380 including nine of the fourteen B cell epitopes in the N protein and one of three B cell epitopes in
381 the M protein predicted by Crooke *et al*.

382 A few other groups have used protein or peptide arrays to map antibody reactivity to SARS-CoV-
383 2 protein (15, 20-23). Two studies included full-length purified structural proteins from SARS-CoV-
384 2, other human coronaviruses and diverse human retroviruses (15, 20). Their results are
385 consistent with ours, but do not include accessory proteins or the ability to map reactive regions
386 in each protein. Several groups used peptides to map epitopes in the SARS-CoV-2 S protein (21-
387 23); Li *et al*. found four epitopes defined by 12 aa peptides, three of which are in regions of
388 antibody reactivity that we found. Poh *et al*. found two epitopes defined by 18 aa peptides. Both
389 are in regions of antibody reactivity that we described here. Finally, Zhang *et al*. used 15 aa
390 peptides overlapping by 5 aa covering the whole SARS-CoV-2 proteome, plus full-length N and
391 E as well as five truncated forms of S to map IgM and IgG responses of acute COVID-19 patients
392 (median 4 days post onset of symptoms). They found a more robust IgM responses, though their
393 specimens were collected earlier during infection. Zhang *et al*. identified five peptides as the most
394 specific for COVID-19 patient IgG binding compared to controls: two in the S protein, two in N and
395 one in ORF-1ab. Both S protein peptides are in regions where we found IgG reactivity; one is in
396 the N-terminal region of reactivity we found in S2 and the other in the central reactivity region of
397 S2. The N peptides of this group were not in a reactive region in our work and we did not assay
398 antibody reactivity of the ORF-1ab polyproteins.

399 Recently two groups published epitope maps of SARS-CoV-2 using phage display (33, 34). One
400 group analyzed 56 aa and 20 aa fragments of the SARS-CoV-2 proteome, while the other group
401 analyzed 38 aa fragments of the proteome. Both studies also included other human coronaviruses
402 and used COVID-19 patient sera and control sera to identify specifically reactive epitopes in the
403 SARS-CoV-2 proteome. Their data are largely in agreement with data presented here. Both
404 studies found the greatest reactivity of COVID-19 patient sera in the S2 and N proteins. Moreover,
405 the epitopes they mapped overlapped with the ones we found here by different methods.

406 On the population level it is clear that groups of SARS-CoV-2 infected subjects have higher
407 antibody levels to the whole N and S2 proteins, but it is also clear that even in the small sample
408 sets evaluated here, some SARS-CoV-2 naïve individuals have substantial pre-existing antibody
409 to some epitopes of these two proteins. Since the pre-existing antibody levels are likely to vary
410 according to many different factors (e.g. geography, age, time of year and associated higher
411 frequency of recent exposure to other coronaviruses) it would be beneficial to have detailed
412 knowledge of specific epitopes of the key immunogenic proteins.

413

414 The multi-coronavirus protein array is a tool that can help us improve our understanding of the
415 immune response to SARS-CoV-2 and other coronaviruses. With these first two sets of
416 convalescent sera provided by the Mayo Clinic and the CDC, we have shown that SARS-CoV-2
417 naïve subjects have clearly measurable cross-reactive antibody to the whole N and S2 proteins
418 and that this reactivity is limited to specific epitopes. Importantly, there are epitopes that are more
419 specific to SARS-CoV-2, that might serve as useful biomarkers of infection. Conversely, we have
420 shown that infection with SARS-CoV-2 elicits or boosts the level of antibodies that bind to the N

421 and S2 proteins of other coronaviruses including SARS-CoV, MERS-CoV, HCoV-NL63 and
422 HCoV-OC43.

423 Limitations of our study are the small sample size and the inclusion of only convalescent samples.
424 Despite these limitations, we were able to identify clear differences in the antibody response from
425 COVID-19 patients and healthy, non-exposed controls. The ideal dataset to further investigate
426 associations between preexisting antibody to specific epitopes and protection from severe
427 disease would be longitudinal, with at least a pre-exposure sample, an acute sample, and a
428 convalescent sample from each subject. Inclusion of samples from COVID-19 patients with a
429 range of clinical symptoms will also provide an important comparison. In upcoming projects, we
430 are seeking to analyze these types of samples paired with detailed clinical data on disease
431 outcomes ranging from asymptomatic to fatal to further improve our understanding of the complex
432 role antibodies play in SARS-CoV-2 infection. It may also prove interesting to test convalescent
433 plasma samples, especially given the variable results on efficacy that have been reported in the
434 literature (27-30). An assay providing more granular detail on the humoral response in these
435 samples, such as the protein microarray described here, may provide valuable insights into what
436 is happening during these convalescent plasma trials.

437

438 **Methods**

439 **Protein microarray analysis of serum samples**

440 The first generation multi-coronavirus protein microarray, produced by Antigen Discovery, Inc.
441 (ADI, Irvine, CA, USA), included 935 full-length coronavirus proteins, overlapping 100, 50 and 30
442 aa protein fragments and overlapping 13-20 aa peptides from SARS-CoV-2 (WA-1), SARS-CoV,
443 MERS-CoV, HCoV-NL63 and HCoV-OC43. Purified proteins and peptides were obtained from
444 BEI Resources. All these coronavirus proteins were produced in *Escherichia coli* except the
445 SARS-CoV-2 and SARS-CoV S proteins, which were made in Sf9 insect cells and the SARS-
446 CoV-2 RBD, made in HEK-293 cells. Other proteins and protein fragments were expressed using
447 an *E. coli in vitro* transcription and translation (IVTT) system (Rapid Translation System,
448 Biotechrabbit, Berlin, Germany) and printed onto nitrocellulose-coated glass AVID slides (Grace
449 Bio-Labs, Inc., Bend, OR, USA) using an Omni Grid Accent robotic microarray printer (Digilabs,
450 Inc., Marlborough, MA, USA). Microarrays were probed with sera and antibody binding detected
451 by incubation with fluorochrome-conjugated goat anti-human IgG or IgA or IgM (Jackson
452 ImmunoResearch, West Grove, PA, USA or Bethyl Laboratories, Inc., Montgomery, TX, USA).
453 Slides were scanned on a GenePix 4300A High-Resolution Microarray Scanner (Molecular
454 Devices, Sunnyvale, CA, USA), and raw spot and local background fluorescence intensities, spot
455 annotations and sample phenotypes were imported and merged in R (R Core Team, 2017), in
456 which all subsequent procedures were performed. Foreground spot intensities were adjusted by
457 subtraction of local background, and negative values were converted to one. All foreground values
458 were transformed using the base two logarithm. The dataset was normalized to remove
459 systematic effects by subtracting the median signal intensity of the IVTT controls for each sample.
460 With the normalized data, a value of 0.0 means that the intensity is no different than the
461 background, and a value of 1.0 indicates a doubling with respect to background. For full-length
462 purified recombinant proteins and peptide libraries, the raw signal intensity data was transformed
463 using the base two logarithm for analysis.

464

465 **Control Sera and COVID-19 Patient samples**

466 COVID-19 positive and pre-COVID-19 negative control sera provided by the CDC were acquired
467 from commercial laboratories or through partnership with Emory University. Samples were

468 provided with only clinical and demographic information retained. The majority of samples (7/10)
469 were from patients that were not hospitalized with blood collected between 26 and 60 days post
470 symptom onset. Negative control sera were collected pre-COVID-19, in the fall of 2019. This
471 activity was reviewed by CDC and was conducted consistent with applicable federal law and CDC
472 policy (45 C.F.R. part 46, 21 C.F.R. part 56). The COVID-19 positive samples provided by Mayo
473 Clinic were de-identified residual sera from clinical testing with only age and sex information
474 available. The COVID-19 negative samples were collected pre-COVID-19 pandemic, between
475 2005-2012. These samples were from participants in prior Mayo Clinic vaccine studies who had
476 provided informed consent for future use of their biospecimens. The original blood collection was
477 collected through Mayo Clinic IRB-approved protocols. Samples were tested for SARS-CoV-2
478 specific antibodies and the presence of neutralizing antibodies as described below.

479

480 **Enzyme linked immunosorbent assay (ELISA)**

481 CDC provided samples were tested using an enzyme-linked immunosorbent assay (ELISA)
482 against the pre-fusion stabilized ectodomain of SARS-CoV-2 spike protein (31). This validated
483 assay has been shown to have sensitivity and specificity of 96% and 99%, respectively (32).
484 Briefly, plates were coated with purified spike protein and incubated overnight at 4°C followed by
485 37°C incubation steps and subsequent phosphate buffered saline + 0.05% Tween 20 (PBST)
486 washings with: 2.5 X Stabilcoat blocker (Surmodics), 1:25 to 1:1600 diluted serum in 1 X PBST +
487 5% skim milk for 1 h, 1:2000 goat anti-human Ab conjugated to horseradish peroxidase (KPL) for
488 1h, ABTS peroxidase substrate for 30 min. Reactions were then quenched with stop
489 solution. Plates were read at 405 nm and 490 nm, with resulting ODs calculated as 490 nm - 405
490 nm absorbance for each sample *and* minus PBS-only coated wells. Results are reported as a
491 ratio of the calculated sample OD/cut-off threshold OD (signal/threshold, or S/T); values >1.0 are
492 defined as positive. The Mayo Clinic COVID-19 positive samples were tested using an IgG
493 SARS-CoV-2 Spike protein-specific ELISA assay (EuroImmune Inc.) performed according to
494 manufacturer's recommendations. This validated assay has been shown to have sensitivity and
495 specificity of 90% and 100%, respectively (39). Results are reported as a ratio of the sample
496 OD/calibrator OD (signal/calibrator, or S/C); values >1.1 are defined as positive.

497

498 **Neutralization assay**

499 All SARS-CoV-2 microneutralization assays (MNT) were performed following biosafety level-3
500 precautions, using a SARS-CoV-2 clinical isolate. The WA1 strain of SARS-CoV-2 was employed
501 using a modified version of a previously established protocol.²⁷ Vero cell suspensions (ATCC
502 CCL-81) were prepared at $2.2 - 2.5 \times 10^5$ cells/mL in DMEM (Thermo Fisher, catalog 11965118)
503 + 10% fetal bovine serum (FBS, defined, Hyclone catalog SH30070.03, heat-inactivated 56°C for
504 30 min) + 2X antibiotic-antimycotic (Thermo Fisher catalog 15240062) + 2X penicillin-
505 streptomycin (Thermo Fisher catalog 15140122) immediately before use. Sera were 2-fold serial
506 diluted in serum-free DMEM in a 96-well flat bottom plate, from 1:10 – 1:320, in triplicate, to a final
507 volume of 50 µL/well. Fifty µL SARS-CoV-2 was to each well, such that final serum dilution titers
508 ranged from 1:20 – 1:640. After 30 min incubation at 37°C and 5% CO₂, 100 µL of Vero cells in
509 suspension were added to each well, for a final concentration of $2.2 - 2.5 \times 10^4$ cells/well. After
510 5 days cells were stained and fixed with crystal violet fixative (0.15% crystal violet, 2.5% ethanol,
511 11% formaldehyde, 50% PBS, 0.01M pH 7.4). The endpoint concentration at which antibodies
512 were determined to be neutralizing for SARS-CoV-2 infection was the lowest concentration of
513 antibody at which 3 replicate wells were protected against virus infection.

514

515 **Statistical Analysis**

516 Student's t-tests were used for comparison of the individual antibody response means between
517 the positive and negative groups. Comparison of the medians was done using Wilcoxon's rank
518 sum test. The area under the receiver operating characteristics curve (AUC) was calculated to
519 estimate delineation of groups for each antigen. The t-SNE analyses were calculated after 25,000
520 iterations with a perplexity parameter of 30 using the R package Rtsne (35). Comparisons of the
521 proportions of responders to each protein between groups was done using two-proportions z-
522 tests implemented by the 'prop.test' function in R. Correlation between antibody features and
523 between protein microarray and ELISA measurements used Pearson's correlation coefficient (ρ),
524 and association between antibody measurements and sample information such as sex, age and
525 cohort were modeled using linear regression. The association of specific antibody responses with
526 virus neutralization titers was estimated using linear regression with the values below detection
527 levels (<20) coded as zero, or by converting neutralization titers to ordinal values and estimating
528 the proportional odds ratio by ordinal logistic regression, whereby p values were estimated by
529 comparing the t-value against the standard normal distribution. Adjustment for the false discovery
530 rate was performed using the "p.adjust" function in R (36). Data visualization was performed using
531 the circlize (37), ComplexHeatmap (38), ggplot2, heatmap2 and corrplot (39) packages in R.
532 Unadjusted p values were shown in graphics.

533

534 **Acknowledgements**

535 We thank the Laboratory Task Force of the CDC COVID_19 response for their project review and
536 resource support. This research was made possible using samples obtained from the CDC
537 Biorepository.

538 The findings and conclusions in this report are those of the author(s) and do not necessarily
539 represent the official position of the Centers for Disease Control and Prevention. Names of
540 specific vendors, manufacturers, or products are included for public health and informational
541 purposes; inclusion does not imply endorsement of the vendors, manufacturers, or products by
542 the Centers for Disease Control and Prevention or the US Department of Health and Human
543 Services.

544 Competing Interest: DC, AZR, KTK, AO, CH, JE, AS, VH, AAT, GH, JVP and JJC are employees
545 of Antigen Discovery, Inc, a company that commercializes proteome microarray technology. XL
546 and AY are employees of Antigen Discovery, Inc and have an equity interest in the company. SP,
547 MS, SNL, JH, AT, MR, NJT, RBK and MT declared no competing interest.

548 Funding: This work was funded by ADI, Mayo Clinic, and the Centers for Disease Control and
549 Prevention.

550 Author Contributions: DC, AY, XL, JJC, AZR, AO and AAT designed the Multi-coronavirus
551 microarray; AY, XL, JJC, MT, SP, RK designed the study, arranged sample selection and testing;
552 AAT, CH, JVP, JE, VH and AS fabricated the array and performed experiments; MS, SNL, JH, AT,
553 MR, and NJT designed and performed ELISA and neutralization assay experiments. AZR, JJC
554 and AO performed statistical analysis and data visualization; and DC, AZR, JJC, RK, SP, MT and
555 AY wrote and reviewed the manuscript.

556 **References**

557

- 558 1. <https://www.who.int/news-room/detail/08-04-2020-who-timeline---covid-19>
- 559
- 560 2. <https://coronavirus.jhu.edu/map.html>

- 561
- 562 3. Kissler S, Tedijanto C, Goldstein E, Grad Y and Lipsitch M (2020) Projecting transmission
563 dynamics of SARS-CoV-2 through the postpandemic period. *Science*
564 10.1126/science.abb5793
- 565
- 566 4. Verity R et al. (2020) Estimates of the severity of coronavirus disease 2019:
567 a model-based analysis. *Lancet Infect Dis* [https://doi.org/10.1016/S1473-3099\(20\)30243-7](https://doi.org/10.1016/S1473-3099(20)30243-7)
568
- 569 5. Long, Antibody responses to SARS-CoV-2 in patients with COVID-19, 2020
570
- 571 6. Zhao, Antibody responses to SARS-CoV-2 in patients of novel coronavirus disease 2019,
572 2020
573
- 574 7. Yu, Distinct features of SARS-CoV-2-specific IgA response in COVID-19 patients, 2020
575
- 576 8. Guo, Profiling Early Humoral Response to Diagnose Novel Coronavirus Disease (COVID-19),
577 2020
578
- 579 9. Atyeo, Distinct Early Serological Signatures Track with SARS-CoV-2 Survival, 2020
580
- 581 10. McAndrews, Heterogeneous antibodies against SARS-CoV-2 spike receptor binding domain
582 and nucleocapsid with implications on COVID-19 immunity, 2020
583
- 584 11. Yang, Evasion of antibody neutralization in emerging severe acute respiratory syndrome
585 coronaviruses, 2005
586
- 587 12. Jaume-Anti-Severe Acute Respiratory Syndrome Coronavirus Spike Antibodies Trigger
588 Infection of Human Immune Cells via a pH- and Cysteine Protease-Independent Fcγ3R
589 Pathway, 2011
590
- 591 13. Yip, Antibody-dependent infection of human macrophages by severe acute respiratory
592 syndrome coronavirus 2014
593
- 594 14. Brouwer et al., *Science* 369, 643–650 (2020)
595
- 596 15. de Assis R et al., Analysis of SARS-CoV-2 Antibodies in COVID-19 Convalescent Plasma
597 using a Coronavirus Antigen Microarray, <https://doi.org/10.1101/2020.04.15.043364> (2020)
598

- 599 16. Crooke et al., <https://doi.org/10.1038/s41598-020-70864-8> (2020)
- 600
- 601 17. Grifoni et al., *Cell Host & Microbe* 27, 671–680, <https://doi.org/10.1016/j.chom.2020.03.002>
602 (2020)
- 603 18. Feng, Y.-E. et al. Multi-epitope vaccine design using an immunoinformatics approach for
604 2019 novel coronavirus in China, <https://doi.org/10.1101/2020.03.03.962332> (2020)
- 605
- 606 19. Fast E and Chen B, Potential T-cell and B-cell Epitopes of 2019-nCoV,
607 <https://doi.org/10.1101/2020.02.19.955484> (2020)
- 608
- 609 20. Khan S et al., Analysis of Serologic Cross-Reactivity Between Common Human
610 Coronaviruses and SARS-CoV-2 Using Coronavirus Antigen Microarray,
611 <https://doi.org/10.1101/2020.03.24.006544> (2020)
- 612
- 613 21. Li, Linear epitopes of SARS-CoV-2 spike protein elicit neutralizing antibodies in COVID-19
614 patients, <https://doi.org/10.1038/s41423-020-00523-5> (2020)
- 615
- 616 22. Poh C, Potent neutralizing antibodies in the sera of 1 convalescent COVID-19 patients
617 2 are directed against conserved linear epitopes on the SARS-CoV-2 spike 3 protein,
618 <https://doi.org/10.1101/2020.03.30.015461> (2020)
- 619
- 620 23. Zhang X, Proteome-wide analysis of differentially-expressed SARS-CoV-2 antibodies in
621 early COVID-19 infection, <https://doi.org/10.1101/2020.04.14.20064535> (2020)
- 622
- 623 24. Wang Q et al., Immunodominant SARS Coronavirus Epitopes in Humans Elicited both
624 Enhancing and Neutralizing Effects on Infection in Non-human Primates,
625 DOI: 10.1021/acsinfecdis.6b00006 (2016)
- 626
- 627 25. Chandrashekar et al., SARS-CoV-2 infection protects against rechallenge in rhesus
628 macaques. *Science* 369 (6505), 812-817. DOI: 10.1126/science.abc4776 (2020)
- 629
- 630 26. Deng et al., Primary exposure to SARS-CoV-2 protects against reinfection in rhesus
631 macaques. *Science* 369 (6505), 818-823. DOI: 10.1126/science.abc5343 (2020)
- 632
- 633 27. Liu et al., Convalescent plasma treatment of severe COVID-19: a propensity score–matched
634 control study, *Nat Med.* doi: 10.1038/s41591-020-1088-9. (2020)

635

636 28. Wang et al., Evaluation of current medical approaches for COVID-19: a systematic review
637 and meta-analysis. doi:10.1136/ bmjpcare-2020-002554 (2020)

638

639 29. Bakhatawar et al., Convalescent Plasma Therapy and Its Effects On COVID-19 Patient
640 Outcomes: A Systematic Review of Current Literature. Cureus 12(8): e9535. DOI
641 10.7759/cureus.9535 (2020)

642

643 30. Wooding and Bach, Treatment of COVID-19 with convalescent plasma: lessons from
644 pastcoronavirus outbreaks. Clin Microbiol Infect. 2020 26:1436-1446.
645 <https://doi.org/10.1016/j.cmi.2020.08.005>. (2020)

646

647 31. Wrapp D, Wang N, Corbett KS, Goldsmith JA, Hsieh CL, Abiona O, et al. Cryo-EM structure
648 of the 2019-nCoV spike in the prefusion conformation. Science. 2020;367:1260–3.

649

650 32. Freeman B, Lester S, Mills L, et al. Validation of a SARS-CoV-2 spike protein ELISA for use
651 in contact investigations and serosurveillance. bioRxiv. 2020 Apr 25; 2020.04.24.057323.
652 doi: 10.1101/2020.04.24.057323.
653 Preprint. <https://www.biorxiv.org/content/10.1101/2020.04.24.057323v2.full>

654

655 33. Shrock E et al. Viral epitope profiling of COVID-19 patients reveals cross-reactivity and
656 correlates of severity. Science 10.1126/science.abd4250 (2020).

657

658 34. Zamecnik, C et al. ReScan, a Multiplex Diagnostic Pipeline, Pans Human Sera for SARS-
659 CoV-2 Antigens. <https://doi.org/10.1016/j.xcrm.2020.100123> (2020)

660

661 35. Benjamini, Y., and Hochberg, Y. (1995). Controlling the false discovery rate: a practical and
662 powerful approach to multiple testing. *Journal of the Royal Statistical Society Series B*, 57,
663 289–300. <http://www.jstor.org/stable/2346101>.

664

665 36. Gu, Z. (2014) circlize implements and enhances circular visualization in R. Bioinformatics.
666 DOI: [10.1093/bioinformatics/btu393](https://doi.org/10.1093/bioinformatics/btu393)

667

668 37. Gu, Z. (2016) Complex heatmaps reveal patterns and correlations in multidimensional
669 genomic data. DOI: [10.1093/bioinformatics/btw313](https://doi.org/10.1093/bioinformatics/btw313)

670

671 38. Michael Friendly (2002). Corrgrams: Exploratory displays for correlation matrices. The
672 American Statistician, 56, 316–324.

673

674 39. [https://www.fda.gov/medical-devices/coronavirus-disease-2019-covid-19-emergency-use-
authorizations-medical-devices/eua-authorized-serology-test-performance](https://www.fda.gov/medical-devices/coronavirus-disease-2019-covid-19-emergency-use-
675 authorizations-medical-devices/eua-authorized-serology-test-performance)